Coherence of atomic matter-wave fields

E. V. Goldstein, O. Zobay, and P. Meystre

Optical Sciences Center, University of Arizona, Tucson, Arizona 85721
(Received 7 April 1998)

In analogy to Glauber's analysis of optical coherence, we adopt an operational approach to introduce different classes of atomic coherence associated with different types of measurements. For the sake of concreteness we consider specifically fluorescence, nonresonant imaging, and ionization. We introduce definitions of coherence appropriate to them, which we call electronic, density, and field coherence, respectively. We illustrate these concepts in various descriptions of Bose-Einstein condensation, showing that each of these descriptions makes different implicit assumptions on the coherence of the system. We also study the impact of elastic collision on the field and density coherence properties of atom lasers. [S1050-2947(98)01509-1]

PACS number(s): 03.75.−b, 42.50.Ar, 42.50.Ct

I. INTRODUCTION

Quantum optical coherence theory is based on the factorization properties of normally ordered correlation functions of the electric field operator [1]. This is a direct consequence of the fact that most optical experiments detect light by absorption, i.e., by "removing" photons from the light field. But the situation is not so simple in the case of matter-wave fields, and in particular for atomic de Broglie waves. This is because atomic detectors can work in a number of different ways: For instance, one can choose to measure electronic properties of the atoms, or center-of-mass properties, or both. Measurements may or may not remove atoms from the field, hence the role of the annihilation operator is not as central as for light fields.

Due to the added complexity of that situation as compared to the optical case, no unified theory of atomic coherence exists to date. The major objective of this paper is to present a step toward this goal, extending the ideas of optical coherence theory to introduce several types of matter-wave coherence, in particular "field coherence" and "density coherence" [2].

In analogy to Glauber's analysis of optical coherence [1], we adopt an operational approach where different classes of atomic coherence are associated with different types of measurements. For the sake of concreteness we consider specifically three classes of measurements: fluorescence, nonresonant imaging, and ionization. Section II briefly reviews the outcome of these measurements, and introduces definitions of coherence appropriate to them. We call them electronic, density, and field coherence, respectively. In the case of bosonic atoms, field-coherent states are easily seen to correspond to the usual Glauber coherent states [1]. In the single-mode case, density-coherent states are simply given by Fock states, but a more general discussion is required for the multimode case. Section III illustrates these ideas in various descriptions of Bose-Einstein condensates. Section IV further develops the concept of multimode density coherence, which is applied to the case of the atom laser in Sec. V. In this latter example, we illustrate in particular how elastic collisions, while strongly modifying the field coherence of the device, have almost no effect on its density coherence. Finally, Sec. VI is a summary and outlook.

II. FIELD AND DENSITY COHERENCE

A physically appealing operational way to discuss matter-wave coherence relies on the analysis of specific detection schemes, in complete analogy with the optical case. As we shall see, this approach naturally leads to the need to associate different *classes of coherence* with different types of measurements. In addition, it builds useful bridges between concepts familiar in quantum optics and methods of traditional many-body theory.

In this paper we consider for concreteness a bosonic atomic Schrödinger field described by a multicomponent field operator $\hat{\boldsymbol{\Psi}}(\mathbf{r},t)$, with components $\hat{\Psi}_i(\mathbf{r},t)$, $i=1,2,\ldots$. We normally think of the atoms comprising this field as adequately described in the Born-Oppenheimer approximation, so that $\mathbf{r}$ describes their center-of-mass motion and the index i labels various electronic states. For bosonic atoms, one has then

$$[\hat{\Psi}_i(\mathbf{r},t),\hat{\Psi}_j^\dagger(\mathbf{r}',t)]=\delta_{ij}\delta(\mathbf{r}-\mathbf{r}'). \qquad (1)$$

Our goal is to characterize the statistical properties of one or more components of this field. One familiar method involves the detection of light fields interacting with the atomic sample, in the hope that properties of the Schrödinger field can be inferred from it. All of laser spectroscopy relies on this approach, although it is not normally cast in terms of matter-wave fields. Another approach, which we will find useful in some respects, involves ionizing atoms from the sample and studying the properties of the emitted ions or electrons. But this method typically also relies on the interaction of the atoms with a light field. Hence, a generic Hamiltonian describing a measurement scheme for the properties of the atomic Schrödinger field is of the form

$$\mathcal{V}=\sum_{ij}\int d^3r\,\hat{\Psi}_j^\dagger(\mathbf{r})[\mathbf{d}_{ij}\cdot\hat{\mathbf{E}}(\mathbf{r},t)]\hat{\Psi}_i(\mathbf{r}), \qquad (2)$$

where $\hat{\mathbf{E}}(\mathbf{r},t)$ is the electric field operator, $\mathbf{d}_{ij}$ is the dipole matrix element between electronic states i and j, and we have assumed for simplicity that the electric dipole approximation gives an adequate description of the atom-field interaction.

PRA <u>58</u>   2373

We consider the situation where the electromagnetic field consists of a classically populated field mode of amplitude E_0, wave vector $\mathbf{k}_0$, and polarization $\boldsymbol{\epsilon}$, and a series of weakly excited side modes of wave vectors $\mathbf{k}_l$ and polarizations $\boldsymbol{\epsilon}_l$. In that case, the Hamiltonian (2) becomes

$$\mathcal{V} = \sum_{ij,l} \int d^3r \hat{\Psi}_j^\dagger(\mathbf{r}) [\Omega_{ij,0}(\mathbf{r}) e^{i(\mathbf{k}_0 \cdot \mathbf{r} - \omega_0 t)}$$
$$+ i\Omega_{ij,l} a_l e^{i\mathbf{k}_l \cdot \mathbf{r}}] \hat{\Psi}_i(\mathbf{r}) + \text{H.c.}, \tag{3}$$

where we have introduced the Rabi frequencies

$$\Omega_{ij,0}(\mathbf{r}) = d_{ij} E_0(\mathbf{r})(\boldsymbol{\epsilon}_{ij} \cdot \boldsymbol{\epsilon})/\hbar \tag{4}$$

corresponding to the classical driving field and the vacuum Rabi frequencies

$$\Omega_{ij,l} = d_{ij} \mathcal{E}_l (\boldsymbol{\epsilon}_{ij} \cdot \boldsymbol{\epsilon}_l)/\hbar. \tag{5}$$

In these expressions, $\boldsymbol{\epsilon}_{ij}$ is the direction of the atomic dipole of magnitude d_{ij} for the $i \leftrightarrow j$ transition, and $\mathcal{E}_l = [\hbar \omega_l / 2\epsilon_0 V]^{1/2}$ is the "electric field per photon" in mode l.

A. Resonance fluorescence

In resonance fluorescence measurements, one proceeds by shining a laser quasiresonant with an electronic transition $g \leftrightarrow e$, and measuring, e.g., the fluorescence spectrum

$$S(\omega) = \int d\tau e^{-i\omega\tau} \langle \hat{E}^-(\mathbf{r}_0,0) \hat{E}^+(\mathbf{r}_0,\tau) \rangle + \text{c.c.} \tag{6}$$

at the location $\mathbf{r}_0$ of a photodetector. In that expression, $\hat{E}^+(\mathbf{r}_0,t)$ and $\hat{E}^-(\mathbf{r}_0,t)$ are the familiar positive and negative frequency parts of the electric field operator, and we have assumed stationarity to identify the Fourier transform of the first-order correlation function of the field with its spectrum. It is well known that, except for unimportant retardation effects, one has that

$$\hat{E}^+(\mathbf{r}_0,t) \propto \hat{\Psi}_e^\dagger(\mathbf{r}_0,t) \hat{\Psi}_g(\mathbf{r}_0,t), \tag{7}$$

so that

$$S(\omega) \propto \int d\tau e^{-i\omega\tau} \langle \hat{\Psi}_g^\dagger(\mathbf{r}_0,0) \hat{\Psi}_e(\mathbf{r}_0,0) \hat{\Psi}_e^\dagger(\mathbf{r}_0,\tau) \hat{\Psi}_g(\mathbf{r}_0,\tau) \rangle$$
$$+ \text{c.c.} \tag{8}$$

Resonance fluorescence has been studied in considerable detail, both experimentally and theoretically. The resonance fluorescence spectrum of a two-state atom is known to consist of a *coherent* and an *incoherent* contribution. For a perfectly monochromatic excitation laser, the coherent spectrum S_{coh} consists of a δ function at the laser frequency, while the incoherent spectrum is the famous Mollow three-peak spectrum. Mathematically,

$$S_{coh} \propto \int d\tau e^{-i\omega\tau} \langle \hat{\Psi}_g^\dagger(\mathbf{r}_0,0) \hat{\Psi}_e(\mathbf{r}_0,0) \rangle \langle \hat{\Psi}_e^\dagger(\mathbf{r}_0,\tau) \hat{\Psi}_g(\mathbf{r}_0,\tau) \rangle$$
$$+ \text{c.c.} \tag{9}$$

and $S_{inc}(\omega) = S(\omega) - S_{coh}(\omega)$. In physical terms, this means that coherent effects are associated with the *factorized* correlation function

$$\langle \hat{\Psi}_g^\dagger(\mathbf{r}_0,0) \hat{\Psi}_e(\mathbf{r}_0,0) \rangle \langle \hat{\Psi}_e^\dagger(\mathbf{r}_0,\tau) \hat{\Psi}_g(\mathbf{r}_0,\tau) \rangle. \tag{10}$$

These considerations justify defining the "electronic coherence" of the matter field $\hat{\boldsymbol{\Psi}}(\mathbf{r},t)$ in terms of the factorization properties of normally ordered correlation functions of the *field polarization* operator

$$\hat{\Sigma}_-(\mathbf{r},t) \equiv \hat{\Psi}_g^\dagger(\mathbf{r},t) \hat{\Psi}_e(\mathbf{r},t). \tag{11}$$

B. Off-resonant imaging

In contrast to resonance fluorescence, off-resonant imaging involves a strongly detuned electromagnetic field interacting with the atoms in the sample in such a way that it induces only virtual transitions. After adiabatic elimination of the upper electronic state of the atomic transition under consideration, the interaction between the Schrödinger field and the radiation field is described to lowest order in the side modes by the effective Hamiltonian

$$V = \hbar \int d^3r \left[\frac{|\Omega_0(\mathbf{r})|^2}{\delta_0} + \sum_l \left(\frac{\Omega_0(\mathbf{r})\Omega_l^\star}{\delta_0} a_l^\dagger e^{i(\mathbf{k}_0 - \mathbf{k}_l)\cdot\mathbf{r}} + \frac{\Omega_0^\star(\mathbf{r})\Omega_l}{\delta_0} a_l e^{-i(\mathbf{k}_0 - \mathbf{k}_l)\cdot\mathbf{r}} \right) \right] \hat{\Psi}^\dagger(\mathbf{r})\hat{\Psi}(\mathbf{r}), \tag{12}$$

where the atom-field detuning $\delta_0 \equiv \omega_a - \omega_0$ is such that $|\delta_0| \gg |\Omega_0(\mathbf{r})|$, and we have omitted the index labeling the ground-state component of the Schrödinger field, which can now be considered as scalar.

There are a number of ways in which off-resonant imaging can be applied to the determination of specific properties of the Schrödinger field. For instance, one can detect interferences between the classical incident field and scattered light, as in the MIT experiments [3]. This results in a signal

proportional to the density $\langle \hat{\rho}(\mathbf{r},t) \rangle$, where we have introduced the *field density* operator

$$\hat{\rho}(\mathbf{r},t) \equiv \hat{\Psi}^\dagger(\mathbf{r},t) \hat{\Psi}(\mathbf{r},t), \tag{13}$$

whose expectation value is the local density of the sample.

Alternatively, one can measure the spectrum of the scattered light in a fashion familiar from resonance fluorescence

experiments [4]. For side modes initially in a vacuum state, the most important nontrivial contribution to the fluorescence signal $\mathcal{F}$ is proportional to the intensity $|\Omega_0|^2$ of the incident field,

$$
\mathcal{F} = \frac{|\Omega_0|^2}{\delta_0^2} \sum_l |\Omega_l|^2 \int d^3r \, d^3r' \int_t^{t+\Delta t} d\tau \, d\tau'
$$
$$
\times e^{i[(\mathbf{k}_0 - \mathbf{k}_l)\cdot(\mathbf{r}-\mathbf{r}') - (\omega_0-\omega_l)(\tau-\tau')]} \langle \hat{\rho}(\mathbf{r},\tau)\hat{\rho}(\mathbf{r}',\tau')\rangle,
$$
$$(14)$$

and hence is sensitive to the second-order correlation function of the Schrödinger field density. Indeed, it can be shown that any measurement involving the electromagnetic field scattered by the atomic sample under conditions of off-resonant imaging is determined by correlation functions of $\hat{\rho}(\mathbf{r},t)$,

$$
D^{(n)}(x_1, \ldots, x_n) = \langle \hat{\rho}(x_1)\cdots\hat{\rho}(x_n)\rangle, \qquad (15)
$$

where $x_i \equiv (\mathbf{r}_i, t_i)$.

In analogy with the optical case, we therefore define a Schrödinger field as being *density-coherent to order* $\mathcal{N}$ if its density correlation functions $D^{(n)}(x_1, \ldots, x_n)$ factorize for all $n \le \mathcal{N}$. From this definition, it is obvious that single-mode density coherent states are the familiar number states. But the situation is more complex for multimode fields, to which we return in Sec. IV.

C. Ionization

1. Physical model

The reason resonance fluorescence and off-resonant imaging yield signals proportional to correlation functions of bilinear products of components of the Schrödinger field is of course that the electric dipole interaction is itself bilinear in the Schrödinger field operators. This raises the question as to whether it is possible to measure correlation functions of $\hat{\Psi}(\mathbf{r},t)$ itself, as in the case of optical fields. This can be achieved if instead of making measurements on the radiation field, one detects the atoms directly [5,6]. One possible scheme that achieves this goal is the ionization method that we now discuss.

Consider a detector consisting of a tightly focused laser beam that can ionize atoms by inducing transitions from their ground electronic level $|g\rangle$ to a continuum level $|i\rangle$. We are interested in measuring properties of the ground-state com-

ponent $\hat{\Psi}_g(\mathbf{r})$ of this field, which is electric dipole-coupled to continuum states $\hat{\Psi}_i(\mathbf{r})$.

In contrast to the preceding measurement schemes, we are no longer interested in the dynamics of the light field, whose role is merely to ionize the atoms. Rather, one extracts information about the state of the Schrödinger field $\hat{\Psi}_g(\mathbf{r},t)$ by standard atomic physics methods, such as, e.g., the detection of the quasifree electrons of the continuum states. It is therefore sufficient to describe the light field via its (possibly time-dependent) classical Rabi frequencies Ω_i between the levels $|g\rangle$ and $|i\rangle$, so that the atom-field interaction reduces to

$$
\mathcal{V} = \hbar \sum_i \int d^3r \, \Omega_i(\mathbf{r},t)\hat{\Psi}_i^\dagger(\mathbf{r})\hat{\Psi}_g(\mathbf{r})e^{-i\omega_L t} + \text{H.c.} \quad (16)
$$

For ground-state atoms cooled well below the recoil temperature and tightly focused laser beams, the spatial size of the atomic wave function is much larger than the laser spot and we can approximate the electric field $\mathbf{E}(\mathbf{r})$ by $\mathbf{E}(\mathbf{r}) \simeq \mathbf{E}\delta(\mathbf{r}-\mathbf{r}_0)$, so that Eq. (16) becomes

$$
\mathcal{V} = \hbar \sum_i \Omega_i(\mathbf{r}_0,t)\hat{\Psi}_i^\dagger(\mathbf{r_0})\hat{\Psi}_g(\mathbf{r_0})e^{-i\omega_L t} + \text{H.c.} \quad (17)
$$

We assume for simplicity that the center-of-mass wave functions of the continuum states of the atoms are well described by plane waves of momentum $\mathbf{q}$, so that the single-atom Hamiltonian $\mathcal{H}_0$ may be expressed as

$$
\mathcal{H}_0 = \mathcal{H}_g + \sum_{i\mathbf{q}} \mathcal{H}_{i\mathbf{q}}, \qquad (18)
$$

where

$$
\mathcal{H}_{i\mathbf{q}} = \hbar\omega_{iq}b_{i,\mathbf{q}}^\dagger b_{i,\mathbf{q}}. \qquad (19)
$$

Here we expanded $\hat{\Psi}_i(\mathbf{r})$ in plane waves as

$$
\hat{\Psi}_i(\mathbf{r}) = \sum_\mathbf{q} \phi_\mathbf{q}(\mathbf{r})b_{i,\mathbf{q}} \qquad (20)
$$

with $[b_{i,\mathbf{q}}, b_{i',\mathbf{q}'}^\dagger] = \delta_{\mathbf{qq}'}\delta_{ii'}$, and $\omega_{iq} = \hbar\mathbf{q}^2/2M + \omega_i$.

In the following we take the atomic system to be initially in the state

$$
|\psi\rangle = |\{\psi_{i,\mathbf{q}}\}, \psi_g\rangle. \qquad (21)
$$

To first order in perturbation theory and for cw beams, the transition probability away from that state during the time interval Δt is

$$
w \simeq \sum_{i,\mathbf{q},i',\mathbf{q}'} |\Omega_i(\mathbf{r}_0)|^2 \int_t^{t+\Delta t} d\tau \int_t^{t+\Delta t} d\tau' \left[e^{i\omega_L(t-t')}\langle\psi_g|\hat{\Psi}_g^\dagger(\mathbf{r}_0,\tau)\hat{\Psi}_g(\mathbf{r}_0,\tau')|\psi_g\rangle \right.
$$
$$
\times \langle\{\psi_{i,\mathbf{q}}\}|\hat{\Psi}_i(\mathbf{r}_0,\tau)|\{\phi_{i',\mathbf{q}'}\}\rangle\langle\{\phi_{i',\mathbf{q}'}\}|\hat{\Psi}_i^\dagger(\mathbf{r}_0,\tau')|\{\psi_{i,\mathbf{q}}\}\rangle + e^{-i\omega_L(t-t')}\langle\psi_g|\hat{\Psi}_g(\mathbf{r}_0,\tau)\hat{\Psi}_g^\dagger(\mathbf{r}_0,\tau')|\psi_g\rangle
$$
$$
\left. \times \langle\{\psi_{i,\mathbf{q}}\}|\hat{\Psi}_i^\dagger(\mathbf{r}_0,\tau)|\{\phi_{i',\mathbf{q}'}\}\rangle\langle\{\phi_{i',\mathbf{q}'}\}|\hat{\Psi}_i(\mathbf{r}_0,\tau')|\{\psi_{i,\mathbf{q}}\}\rangle \right],
$$
$$(22)$$

where the sum is over all final states $|\{\phi_{i',\mathbf{q}'}\}\rangle$ in the excited state manifold. In this expression, we have neglected contributions involving the product of two creation or annihilation operators, a result of the implicit assumption that any atom in the continuum will be removed from the sample instantaneously. In addition, we explicitly carried out the sum over all final states of the ground-state field, but not for the excited fields manifold. This is because we want to allow for the possibility of selective detection of the ionized atoms. Following Ref. [1], this can be easily achieved by replacing the sum over final states in Eq. (22) by a weighted sum

$$\sum_{i',\mathbf{q}'} \rightarrow \sum_{i',\mathbf{q}'} \mathcal{R}(i',\mathbf{q}'), \tag{23}$$

where $\mathcal{R}(i',\mathbf{q}')$ is the detector sensitivity to atoms in state $|\phi_{i',\mathbf{q}'}\rangle$. In practice, we have in mind energy-selective detectors, $\mathcal{R}(i',\mathbf{q}') \rightarrow \mathcal{R}(\omega)$, and the degeneracy of the levels must then of course be accounted for.

There is a fundamental distinction between the situation at hand and Glauber's photodetection theory, because in the present case both the detected and detector fields consist of matter waves. There is a complete symmetry between these two fields so far, and their roles are interchangeable. In order to break this symmetry and to truly construct a detector, we now make a series of assumptions on the state of the detector fields $\hat{\Psi}_i(\mathbf{r},t)$. Physically, this amounts to making a statement about the way the detector is prepared prior to a measurement. Specifically, we assume that all atoms are in the ground state, $\Psi_i(\mathbf{r}_0,0)|\{\psi_{i,\mathbf{q}}\}\rangle = 0$, and that any atom in an ionized state will be removed from the sample instantaneously, as already mentioned. In that case, the second term in Eq. (22) vanishes.

2. Energy-selective detectors

To illustrate this result, we consider the situation of energy-selective detectors, and discuss the limits of *narrow-band* and *broadband* detection [1,7]. In the first case the detector bandwidth ΔE_d is assumed to be much narrower than the energy width ΔE_g of the ground-state Schrödinger field, which is determined solely by the spread in center-of-mass momentum (temperature) since all atoms occupy the same internal state. The reverse is true in the second case. We note that in contrast to the detection of optical fields, where the center-of-mass motion of the detector is ignored, the narrowband regime can now be achieved only by manipulating the detector sensitivity $\mathcal{R}(E)$. This is because even a monochromatic excitation of the atomic fields results in equal bandwidths $\Delta E_g = \Delta E_d$ of the detected and detector fields, due to atomic center-of-mass dispersion.

For a narrowband detector and long enough detection times $\Delta t \gg \hbar/\Delta E_g$, the substitution of Eq. (23) into Eq. (22) yields readily

$$r_{nb}(\omega) \sim \int_{-\infty}^{\infty} d\tau e^{-i(\omega-\omega_L)\tau} G_A(t,t+\tau;\mathbf{r}_0,\mathbf{r}_0) + \text{c.c.} \tag{24}$$

Here $\hbar\omega$ is the energy of the registered photoelectrons, and we introduced the ionization rate $r_{nb}(\omega) = w_{nb}(\omega)/\Delta t$ and the normally ordered first-order correlation function of the ground-state Schrödinger field $G_A(t,t';\mathbf{r}_0,\mathbf{r}_0) = \langle\hat{\Psi}_g^\dagger(\mathbf{r}_0,t)\hat{\Psi}_g(\mathbf{r}_0,t')\rangle$. In this limit, the detector measures the Fourier component of the atomic correlation function $G_A(t,t';\mathbf{r}_0,\mathbf{r}_0)$. For stationary fields, the Wiener-Khintchine theorem implies that tuning the detector sensitivity $\mathcal{R}(E)$ yields the spectrum of the Schrödinger field $\hat{\Psi}_g(\mathbf{r},0)$.

In the case of broadband detection, in contrast, the energy distribution ΔE_d of the ionized states is much broader than ΔE_g. This situation can be realized, e.g., by exciting the ground state with a broadband laser pulse and detecting the resulting electrons (or ions) with a broadband detector $\mathcal{R}(E) \simeq$ const. Assuming that the spectrum of the ground atoms Schrödinger field is centered at $\bar{\omega}$, we find

$$r_{bb} \simeq \eta(\mathbf{r}_0) G_A(t,t;\mathbf{r}_0,\mathbf{r}_0), \tag{25}$$

where we have introduced in prevision of the following discussion the "detector cross-efficiency"

$$\eta(\mathbf{r}_1,\mathbf{r}_2) = \sum_i \Omega_i(\mathbf{r}_1)\Omega_i^\star(\mathbf{r}_2)$$
$$\times \int_0^{\Delta t} d\tau \langle\hat{\Psi}_i(\mathbf{r}_2,t+\tau)\hat{\Psi}_i^\dagger(\mathbf{r}_1,t)\rangle e^{-i(\bar{\omega}-\omega_L)\tau}, \tag{26}$$

from which the usual detector efficiency is simply recovered as $\eta(\mathbf{r}_0) \equiv \eta(\mathbf{r}_0,\mathbf{r}_0)$. As expected, a broadband detector is not able to resolve any spectral feature of the Schrödinger field, and only measures the local atomic density, like off-resonant imaging.

3. Higher-order correlations

The detection of higher-order correlations of the Schrödinger field can be achieved by a straightforward generalization of the ionization detector. For instance, second-order coherence measurements can be carried out by focusing the laser at two locations $\mathbf{r}_1$ and $\mathbf{r}_2$, in which case

$$\mathcal{V} = \hbar \sum_{\mu=1,2} \sum_j \Omega_j(\mathbf{r}_\mu)\hat{\Psi}_j^\dagger(\mathbf{r}_\mu)\hat{\Psi}_g(\mathbf{r}_\mu) e^{-i\omega_L t} + \text{H.c.}$$

The joint probability to ionize an atom at $\mathbf{r}_1$ and another one at $\mathbf{r}_2$ is then

$$w_2 \simeq \sum_{\{j_i\}\{\mathbf{q}_i\}} \int_t^{t+\Delta t} d\tau_1 \int_t^{t+\Delta t} d\tau_2 \int_t^{t+\Delta t} d\tau_3 \int_t^{t+\Delta t} d\tau_4 e^{-i\omega_L(\tau_1+\tau_2-\tau_3-\tau_4)} \Omega_{j_1}^\star(\mathbf{r}_1)\Omega_{j_2}^\star(\mathbf{r}_2)\Omega_{j_3}(\mathbf{r}_2)\Omega_{j_4}(\mathbf{r}_1)$$
$$\times \langle\hat{\Psi}_{j_1}(\mathbf{r}_1,\tau_1)\hat{\Psi}_{j_2}(\mathbf{r}_2,\tau_2)\hat{\Psi}_{j_3}^\dagger(\mathbf{r}_2,\tau_3)\hat{\Psi}_{j_4}^\dagger(\mathbf{r}_1,\tau_4)\rangle\langle\hat{\Psi}_g^\dagger(\mathbf{r}_1,\tau_1)\hat{\Psi}_g^\dagger(\mathbf{r}_2,\tau_2)\hat{\Psi}_g(\mathbf{r}_2,\tau_3)\hat{\Psi}_g(\mathbf{r}_1,\tau_4)\rangle. \tag{27}$$

It involves two detected atoms, hence it is now necessary to properly account for the quantum statistics of the measured particles. For this purpose, we describe the ionized atoms as ion-electron pairs, whereby the electrons are described by the creation and annihilation operators $c_{\mathbf{k}s}^{\dagger}$ and $c_{\mathbf{k}s}$ satisfying Fermi commutation relations $[c_{\mathbf{k}s}, c_{\mathbf{k}'s'}^{\dagger}]_{+} = \delta_{ss'}\delta_{\mathbf{kk}'}$. Here s labels the electron spin and $\mathbf{k}$ its momentum. We similarly introduce ion creation and annihilation operators $a_{\mathbf{k}s}^{\dagger}, a_{\mathbf{k}s}$, also satisfying Fermi commutation relations (for bosonic atoms.) For a spin-zero atom, the atomic mode operators $b_{j,\mathbf{q}}$ can be expressed in terms of the ion and electron operators as

$$b_{j,\mathbf{q}} \equiv |j\mathbf{q}\rangle\langle 0| = \sum_{\mathbf{kk}'ss'} |\mathbf{kk}'ss'\rangle\langle\mathbf{kk}'ss'|j\mathbf{q}\rangle\langle 0|$$

$$= \sum_{\mathbf{k}s} \varphi_j(\mathbf{k}) a_{\mathbf{q}s} c_{\mathbf{k}-s} = \sum_{s} a_{\mathbf{q}s} c_{j-s}, \tag{28}$$

where $\varphi_j(\mathbf{k})$ are electron wave functions in $\mathbf{k}$ space, $c_{js} = \Sigma_{\mathbf{k}}\varphi_j(\mathbf{k})c_{\mathbf{k}s}$, and we have assumed that the center-of-mass wave function is $e^{i\mathbf{q}\cdot\mathbf{r}}$ with $\mathbf{r}$ being the ion (or atomic center-of-mass) position. Due to spin conservation the values of electron and ion spins are clearly opposite.

Substituting this result into Eq. (27) yields, in the case of broadband detection,

$$w_2 = \eta(\mathbf{r}_1)\eta(\mathbf{r}_2)\int_t^{t+\Delta t} d\tau_1 \int_t^{t+\Delta t} d\tau_2 \langle \Phi_g^{\dagger}(\mathbf{r}_1,\tau_1)\Phi_g^{\dagger}(\mathbf{r}_2,\tau_2)\Phi_g(\mathbf{r}_2,\tau_2)\Phi_g(\mathbf{r}_1,\tau_1)\rangle$$

$$+ \eta(\mathbf{r}_1,\mathbf{r}_2)\eta(\mathbf{r}_2,\mathbf{r}_1)\int_t^{t+\Delta t} d\tau_1 \int_t^{t+\Delta t} d\tau_2 \langle \Phi_g^{\dagger}(\mathbf{r}_1,\tau_1)\Phi_g^{\dagger}(\mathbf{r}_2,\tau_2)\Phi_g(\mathbf{r}_2,\tau_1)\Phi_g(\mathbf{r}_1,\tau_2)\rangle$$

$$+ \eta_x(\mathbf{r}_1,\mathbf{r}_2)\int_t^{t+\Delta t} d\tau_1 \langle \Phi_g^{\dagger}(\mathbf{r}_1,\tau_1)\Phi_g^{\dagger}(\mathbf{r}_2,\tau_1)\Phi_g(\mathbf{r}_2,\tau_1)\Phi_g(\mathbf{r}_1,\tau_1)\rangle, \tag{29}$$

where the detector sensitivity $\eta_x(\mathbf{r}_1,\mathbf{r}_2)$ to processes involving electron exchange is

$$\eta_x(\mathbf{r}_1,\mathbf{r}_2) = \int_t^{t+\Delta t} d\tau_2 \int_t^{t+\Delta t} d\tau_3 \int_t^{t+\Delta t} d\tau_4 e^{-i\omega_L(\tau_1+\tau_2-\tau_3-\tau_4)} \sum_{\alpha\beta\kappa\mathbf{q}} [e^{i[\omega_\kappa(\tau_1-\tau_3)+\omega_q(\tau_2-\tau_4)+\omega_\alpha(\tau_1-\tau_4)+\omega_\beta(\tau_2-\tau_3)]}$$

$$\times |\Omega_\alpha(\mathbf{r}_1)|^2 |\Omega_\beta(\mathbf{r}_2)|^2 \phi_\kappa^{\star}(\mathbf{r}_1)\phi_\kappa(\mathbf{r}_2)\phi_{\mathbf{q}}^{\star}(\mathbf{r}_2)\phi_{\mathbf{q}}(\mathbf{r}_1) + \Omega_\alpha^{\star}(\mathbf{r}_1)\Omega_\alpha(\mathbf{r}_2)\Omega_\beta^{\star}(\mathbf{r}_2)\Omega_\beta(\mathbf{r}_1)|\phi_\kappa(\mathbf{r}_1)|^2 |\phi_{\mathbf{q}}(\mathbf{r}_2)|^2$$

$$\times e^{i[\omega_\kappa(\tau_1-\tau_4)+\omega_q(\tau_2-\tau_3)+\omega_\alpha(\tau_1-\tau_3)+\omega_\beta(\tau_2-\tau_4)]}]. \tag{30}$$

The first term in Eq. (29) is familiar from double photodetection, with the usual exchange contributions from the *detected* field. The second term is an additional exchange term due to the fact that the detector field is a single Schrödinger field. Its origin is the interference of the *detector* field at points $\mathbf{r}_1$ and $\mathbf{r}_2$. It is absent in conventional photodetection theory, a result of the implicit assumption that the two detectors used are distinguishable.[1] Finally, the term proportional to η_x results from the fact that electrons do not know from which atom they originate. We note that these last two terms can be eliminated by using a gated detection scheme [7] that eliminates the contribution of the exchange terms in the detector field. In practice, such gating can be achieved by using nonoverlapping short laser pulses to ionize the atoms.

---

[1] A similar comment can be made about the position measurement scheme discussed in Refs. [5,6]. In that case, the absence of the detector exchange contribution can be traced back to the assumption that the sets of states excited at different locations are distinguishable. While this approximation is usually reasonable, it becomes questionable in situations involving quantum degenerate gases such as Bose-Einstein condensates.

In that case, the ionization scheme simply yields normally ordered correlation functions of the Schrödinger field

$$G^{(n)}(x_1, \ldots, x_n) = \langle \hat{\Psi}^{\dagger}(x_1)\cdots\hat{\Psi}^{\dagger}(x_n)\hat{\Psi}(x_n)\cdots\hat{\Psi}(x_1)\rangle, \tag{31}$$

in complete analogy with the optical situation. This also justifies defining a Schrödinger field as *field coherent to order* $\mathcal{N}$ if its normally ordered correlation functions $G^{(n)}$ factorize for all $n \leq \mathcal{N}$.

III. EXAMPLE: BOSE-EINSTEIN CONDENSATION

A. Hartree description

To illustrate the ideas developed in the preceding section, we consider a quantum-degenerate N-particle bosonic system described by the state

$$|\psi(t)\rangle_N = \frac{1}{\sqrt{N!}} \int d\{\mathbf{r}_i\} f_N(\{\mathbf{r}_i\},t)\Pi_i\hat{\Psi}^{\dagger}(\mathbf{r}_i)|0\rangle, \tag{32}$$

where the N-body wave function $f_N(\{\mathbf{r}_i\},t)$ is totally symmetric in its arguments. If the sample forms a condensate, it

is described to an excellent degree of approximation by a Hartree wave function, whereby the N-body wave function $f_N(\{\mathbf{r}_i\},t)$ factorizes as a product of the form $f_N(\{\mathbf{r}_i\},t) = \Pi_i \phi_N(\mathbf{r}_i,t)$. That is, all atoms in the condensate are described by the same Hartree wave function $\phi_N(\mathbf{r},t)$ and the N-particle state reduces to

$$|\psi(t)\rangle_N = \frac{1}{\sqrt{N!}}\left(\int d\mathbf{r}\,\phi_N(\mathbf{r},t)\hat{\Psi}^\dagger(\mathbf{r})\right)^N|0\rangle. \quad (33)$$

The equation of motion for $\phi_N(\mathbf{r},t)$ is obtained from the variational principle

$$\frac{\delta}{\delta\phi_N^\star(\mathbf{r})}\left[{}_N\langle\psi|i\hbar\frac{\partial}{\partial t}-\mathcal{H}|\psi\rangle_N\right]=0, \quad (34)$$

where $\mathcal{H}$ is a many-body Hamiltonian.

We expand then the Schrödinger field as[2] [8]

$$\hat{\Psi}^\dagger(\mathbf{r}) = \phi_N^\star(\mathbf{r})a^\dagger + \delta\hat{\psi}^\dagger(\mathbf{r}), \quad (35)$$

where $a^\dagger$ is the creation operator for a particle with the Hartree wave function $\phi_N(x)$ and the operator $\delta\hat{\psi}^\dagger(\mathbf{r})$ creates particles in all other states. Further assuming that the condensate state is stationary

$$\phi_N(\mathbf{r},t) = \phi_N(\mathbf{r})e^{-i\mu_N t/\hbar} \quad (36)$$

with μ_N being the chemical potential, the state of the system is simply

$$|\psi(t)\rangle_N = \frac{e^{-i\mu_N t/\hbar}}{\sqrt{N!}}(a^\dagger)^N|0\rangle \equiv |N\rangle, \quad (37)$$

where we have used the orthogonality of the condensate state to all other modes, i.e., $\int d\mathbf{r}\,\phi_N(\mathbf{r})\,\delta\psi^\dagger(\mathbf{r})|0\rangle = 0$. Hence the Hartree approximation is equivalent to the assumption that the condensate is in a number state of the self-consistent Hartree ''mode.'' In this description the condensate is in a density coherent state (37). Indeed, $|\psi(t)\rangle_N$ is easily seen to be an eigenstate of the field density operator $\hat{\rho}(\mathbf{r})$,

$$\hat{\rho}(\mathbf{r})|\psi(t)\rangle_N = N\rho(\mathbf{r})|\psi(t)\rangle_N, \quad (38)$$

where $\rho(\mathbf{r})=|\phi_N(\mathbf{r})|^2$ is the local Hartree density of the condensate. It is straightforward to see that this state is density-coherent to all orders. However, just like single-mode number states of the electromagnetic field, it does not exhibit *field* coherence past first-order coherence.

B. Wave-packet description

For small systems containing a finite number of atoms, the assumption that all particles are in the condensate state is actually not realistic. Rather, the particle number in a condensate fluctuates, so that only the mean number of atoms in the condensate is known. In this picture it is appropriate to describe the condensate as a wave packet in Fock space, and assume that the particle number distribution is sharply peaked around $\bar{N}$. Following Ref. [8] we assume a Poissonian particle number distribution, and thus, the state of a condensate reads

$$|\psi(t)\rangle = e^{-\bar{N}}\sum_N \frac{\bar{N}^{N/2}}{N!}e^{-iN\mu_N t/\hbar}(a^\dagger)^N|0\rangle. \quad (39)$$

In contrast to a pure condensate state with a fixed number of atoms in the Hartree ground state, this state can be characterized with a nonzero ''order parameter'' defined by [8]

$$\Phi(\mathbf{r},t) \equiv \langle\psi(t)|\Psi(\mathbf{r})|\psi(t)\rangle = \sqrt{\bar{N}}\phi_{\bar{N}}(\mathbf{r})e^{-i\mu t/\hbar}\mathcal{F}_N(t), \quad (40)$$

where $\mu = \mu_{\bar{N}} + \bar{N}\mu_N'$, $\mu_N' \equiv \partial\mu_N/\partial N|_{N=\bar{N}}$ and

$$\mathcal{F}_N(t) = e^{-\bar{N}}\sum_N \frac{\bar{N}^{(N-1)}}{(N-1)!}e^{-2i\mu_N'(N-\bar{N})t/\hbar}. \quad (41)$$

This order parameter exhibits periodical collapses and revivals due to the dispersion of the chemical potential over the particle number variance. Physically, this is a consequence of the fact that while the initial state of the condensate is field (Glauber) coherent, it does not remain so in the course of time. Hence, the state (39) is neither field nor density coherent.

Interestingly, it turns out that the *one-time* field coherence functions measured in ionization experiments (Sec. II C) are factorizable. Indeed, the first-order field coherence function in this case reads

$$G^{(1)}(\mathbf{r};0) = \bar{N}|\phi_{\bar{N}}(\mathbf{r})|^2$$

and the second-order field coherence function is

$$G^{(2)}(\mathbf{r},\mathbf{r}';0) = \bar{N}^2|\phi_{\bar{N}}(\mathbf{r})|^2|\phi_{\bar{N}}(\mathbf{r}')|^2,$$

so that the normalized second-order coherence function $g^{(2)}(0)=1$.

C. Spontaneous symmetry breaking description

As a final possible description of the condensate, we consider the standard spontaneous symmetry breaking approach whereby the Schrödinger field operator is replaced by a c number [9],

$$\hat{\Psi}(\mathbf{r},t) \rightarrow \Phi(\mathbf{r},t). \quad (42)$$

This description is equivalent to the assumption that the state of the system is an eigenstate of the Schrödinger field operator $\hat{\Psi}(\mathbf{r},t)|\psi\rangle = \Phi(\mathbf{r},t)|\psi\rangle$, or, in other words, that the condensate is in a Glauber coherent state. This state can be obtained from the previous wave packet description in the thermodynamic limit when the dispersion of μ over the par-

---

[2]Note that this representation of the Schrödinger field operator is different from the Bogoliubov description, a consequence of the fact that the system is *not* taken to be in a field coherent state.

ticle number variance becomes negligible and μ_N can be approximated by $\mu_{\bar{N}}$. In that case

$$\Phi(\mathbf{r},t)|\psi\rangle = \sqrt{\bar{N}}e^{-i\mu_{\bar{N}}t}\phi_{\bar{N}}(\mathbf{r})|\psi\rangle, \qquad (43)$$

the condensate remains in a Glauber coherent state at all times. It is field coherent, but not density coherent since for that state one finds easily that

$$D^{(2)}(\mathbf{r},\mathbf{r}';0) = D^{(1)}(\mathbf{r})D^{(1)}(\mathbf{r}') + D^{(1)}(\mathbf{r})\delta(\mathbf{r}-\mathbf{r}'). \qquad (44)$$

These results illustrate how different descriptions of the condensate make different implicit assumptions about its coherence properties. These models are amenable, at least in principle, to experimental tests. We note finally that all descriptions reviewed in this section become equivalent in the thermodynamic limit as far as their coherence properties are concerned, despite the fact that their order parameters are different.

IV. MULTIMODE DENSITY CORRELATIONS

A. Density-coherent states

In this section we further develop the notion of density coherence and introduce density-coherent states for a multimode Schrödinger field.[3]

From the definition (15) of the nth-order density correlation function, we have readily that

$$D^{(n)}(x_1,\ldots,x_n) = D^{(n)}(x_n,\ldots,x_1)^*. \qquad (45)$$

If all x_i are taken at the same time, $D^{(n)}$ is real. Similarly to the case of field correlation functions [10] one can derive the inequality

$$\begin{aligned} D^{(2n)}(x_1,&\ldots,x_n,x_n,\ldots,x_1) \\ &\times D^{(2m)}(y_m,\ldots,y_1,y_1,\ldots,y_m) \\ &\geq |D^{(m+n)}(x_1,\ldots,x_n,y_1,\ldots,y_m)|^2. \end{aligned} \qquad (46)$$

The state of a system is said to be $\mathcal{N}$th-order density coherent if all density correlation functions up to order $\mathcal{N}$ factorize, i.e.,

$$D^{(n)}(x_1,\ldots,x_n) = D^{(1)}(x_1)\cdots D^{(1)}(x_n), \quad n\leq\mathcal{N}, \qquad (47)$$

where we recall that $D^{(1)}(x)$ is nothing but the expectation value of the Schrödinger field density, see Eq. (15).

Disregarding mathematical rigor, states that are density coherent if all x_i are taken at the same time can be constructed as follows. Define

$$|y_m,\ldots,y_1\rangle = \frac{1}{\sqrt{\mathcal{C}}}\hat{\Psi}^\dagger(y_m)\cdots\hat{\Psi}^\dagger(y_1)|0\rangle \qquad (48)$$

with $\mathcal{C} = \langle 0|\hat{\Psi}(y_1)\cdots\hat{\Psi}(y_m)\hat{\Psi}^\dagger(y_m)\cdots\hat{\Psi}^\dagger(y_1)|0\rangle$.[4] This state describes a system of m particles that are localized at points $y_1,\ldots,y_m$. For this state the density correlation functions are of the form (47) with

$$D^{(1)}(x) = \sum_{i=1}^m \delta(x-y_i), \qquad (49)$$

which is a direct consequence of the relation

$$\hat{\rho}(x)|y_m,\ldots,y_1\rangle = \left[\sum_{i=1}^m \delta(x-y_i)\right]|y_m,\ldots,y_1\rangle. \qquad (50)$$

Due to dispersion the states $|y_m,\ldots,y_1\rangle$ will not remain density coherent in the course of time.[5]

For the sake of comparison we also compute the equal-time first-order correlation function for a general two-particle state

$$|\phi\rangle = \frac{1}{\sqrt{2}}\int dx_1 dx_2\, \phi(x_1,x_2)\hat{\Psi}^\dagger(x_1)\hat{\Psi}^\dagger(x_2)|0\rangle \qquad (51)$$

with symmetric two-particle wave function $\phi(x_1,x_2)$. Denoting the marginal distribution $\int dx_2|\phi(x_1,x_2)|^2$ by $p(x_1)$ one obtains

$$D^{(1)}(x_1,x_2) = 2|\phi(x_1,x_2)|^2 + 2p(x_1)\delta(x_1-x_2), \qquad (52)$$

compared with Eq. (44). This correlation function is not factorizable in general.

B. Thermal fields

A simple system that can be discussed in the context of density correlations is provided by the thermal multimode Schrödinger field. Here for the sake of simplicity we consider an ideal thermal Bose gas of atoms without condensate fraction (i.e., above the Bose condensation transition temperature T_c)[6] in which case the state of the system is described by the density operator

---

[3]The discussion in this section can also be applied to a more general class of density correlation functions. To this end, consider a one-particle observable $\mathcal{B}$ with (discrete or continuous) eigenvalues b_n and eigenvectors $|b_n\rangle$. One might choose $\mathcal{B}=\mathbf{p}$, for example. In analogy to $\hat{\Psi}^\dagger(\mathbf{r},t)$ and $\hat{\rho}(\mathbf{r},t)$ one can construct operators $\hat{\Psi}^\dagger(b_n,t)$ and $\hat{\rho}(b_n,t)$. In terms of these operators one defines density correlation functions according to Eq. (15). The subsequent derivations then apply similarly to these correlations functions. In case of B having a discrete spectrum, the mathematical problems connected with the normalizability of the density-coherent states do not arise.

[4]The normalization constant $\mathcal{C}$ is not well defined mathematically, of course. This is due to the continuous nature of the eigenvalue spectrum of the position operator $\hat{\mathbf{r}}$. If one considered density correlation functions for a discrete operator $\mathcal{B}$ (as outlined in the previous footnote) these problems would not arise.

[5]However, the momentum eigenstates will be ''momentum density coherent'' at all times for free particles, i.e., if $H=\mathbf{p}^2/2m$.

[6]The calculation of the second-order field coherence function for the thermal Bose gas with both interactions and condensate fraction present can be found in [11].

$$\hat{\rho}_T = \frac{1}{Z} e^{-\sum_k (\epsilon_k - \mu) a_k^\dagger a_k / k_B T}, \quad (53)$$

where ϵ_k is the eigenenergy of the kth mode, k_B the Boltzmann constant, T is temperature, μ the chemical potential, and Z the partition function. The equal-time first-order field coherence function of this system is

$$G^{(1)}(x) = \text{Tr}[\hat{\rho}_T \hat{\Psi}^\dagger(x) \hat{\Psi}(x)] = \sum_k \overline{n_k} |\phi_k(x)|^2, \quad (54)$$

where we have expanded the Schrödinger field operator in terms of mode annihilation operators in the usual way as $\hat{\Psi}(x) = \Sigma_k \phi_k(x) a_k^\dagger$, and the mean number of atoms in mode k is $\overline{n}_k = \text{Tr}(\hat{\rho}_T a_k^\dagger a_k)$. Similarly, the equal-time second-order field coherence function is

$$G^{(2)}(x_1, x_2) = \text{Tr}[\hat{\rho}_T \hat{\Psi}^\dagger(x_1) \hat{\Psi}^\dagger(x_2) \hat{\Psi}(x_2) \hat{\Psi}(x_1)]$$

$$= \sum_{k_1 k_2} \overline{n}_{k_1} \overline{n}_{k_2} [|\phi_{k_1}(x_1)|^2 |\phi_{k_2}(x_2)|^2$$

$$+ \phi_{k_1}^\star(x_1) \phi_{k_1}(x_2) \phi_{k_2}^\star(x_2) \phi_{k_2}(x_1)].$$
$$(55)$$

These correlation functions are not factorizable. The one-point normalized second-order coherence function is

$$g^{(2)}(x) \equiv G^{(2)}(x,x)/G^{(1)}(x)G^{(1)}(x) = 2. \quad (56)$$

The equal-time second-order density coherence function is

$$D^{(2)}(x_1, x_2) = \text{Tr}[\hat{\rho}_T \hat{\Psi}^\dagger(x_1) \hat{\Psi}(x_1) \hat{\Psi}^\dagger(x_2) \hat{\Psi}(x_2)]$$

$$= G^{(2)}(x_1, x_2) + G^{(1)}(x_1) \delta(x_1 - x_2) \quad (57)$$

and is likewise not factorizable. Thus the thermal Schrödinger field is neither field nor density coherent.

V. FIELD VERSUS DENSITY COHERENCE IN A DYNAMICAL SYSTEM: THE BINARY-COLLISION ATOM LASER

In order to illustrate how differently the field and density coherence of a Schrödinger field can behave in a dynamical system, we compute these properties for a model of a binary-collision atom laser. We show in particular that elastic collisions, while being extremely detrimental to the field coherence, and hence to the linewidth of the laser, have almost no influence on its density coherence.

This binary-collision atom laser has been investigated in various publications [12–17]. One considers a resonator for atoms, realized, e.g., by optical fields, in which only three atomic center-of-mass modes are taken into account explicitly (cf. Fig. 1). Bosonic atoms in their ground electronic state are pumped into an atomic resonator level of ''intermediary'' energy (mode 1). They then undergo binary collisions that take one of the atoms involved to the tightly bound laser mode 0, whereas the other one is transferred to the heavily damped loss mode 2. This latter atom leaves the resonator quickly, thereby providing the irreversibility of the pumping process. A macroscopic population of the laser mode can
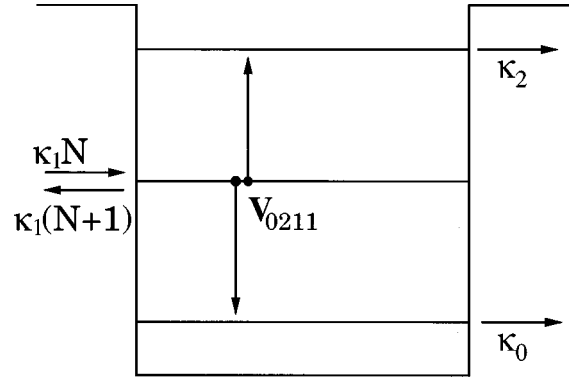

FIG. 1. Schematic three-mode atom laser model.

build up as soon as the influx of atoms due to pumping compensates for the losses induced by the damping.

For the master equation of this atom laser model one makes the ansatz

$$\dot{W} = -i[H_0 + H_{\text{col}}, W] + \kappa_0 \mathcal{D}[a_0]W + \kappa_1(N+1)\mathcal{D}[a_1]W$$

$$+ \kappa_1 N \mathcal{D}[a_1^\dagger]W + \kappa_2 \mathcal{D}[a_2]W \quad (58)$$

with $\hbar = 1$. In this equation, the second quantized formalism is used in which each center-of-mass atomic mode is associated with an annihilation operator a_i, and W denotes the atomic density operator.[7] The free Hamiltonian is given by

$$H_0 = \sum_{i=0,1,2} \omega_i a_i^\dagger a_i,$$

ω_i being the mode frequencies. For the following we set $\omega_0 + \omega_2 = 2\omega_1$. This condition can be fulfilled, e.g., if the atomic cavity is realized by time-modulated optical fields [15].

The operation of the atom laser relies on binary collisions between the atoms in the resonator. The general form of the corresponding interaction Hamiltonian is

$$H_{\text{col}} = \sum_{i \leq j, k \leq l} V_{ijkl} a_i^\dagger a_j^\dagger a_k a_l, \quad (59)$$

where V_{ijkl} are the matrix elements of the two-body interaction responsible for the collisions. However, for the present investigation we restrict our attention to the simplified form

$$H_{\text{col}} = V_{0211} a_0^\dagger a_2^\dagger a_1 a_1 + V_{1102} a_1^\dagger a_1^\dagger a_0 a_2 + V_{0000} a_0^\dagger a_0^\dagger a_0 a_0 \quad (60)$$

in which (besides the pumping collisions) only collisions involving ground-state atoms are retained. The damping rates of the cavity modes are given by the coefficients κ_i, and the strength of the external pumping of mode 1 is characterized by the parameter N, which is the mean number of atoms to which mode 1 would equilibrate in the absence of collisions. The superoperator $\mathcal{D}$ is of the Lindblad form and is defined by

---

[7]Since we consider ground-state atoms only, they are fully described by their center-of-mass quantum numbers.

$$\mathcal{D}[c]P = cPc^\dagger - \frac{1}{2}(c^\dagger c P + P c^\dagger c) \qquad (61)$$

with arbitrary operators c and P.

In order to achieve a sufficiently high degree of irreversibility, it is necessary that κ_2 is much larger than the damping rates of the other modes. This suggests to adiabatically eliminate this mode, an approximation that leads to the simplified master equation [12–14]

$$\dot\rho = -i[H_c, \rho] + \kappa_0 \mathcal{D}[a_0]\rho + \kappa_1(N+1)\mathcal{D}[a_1]\rho$$
$$+ \kappa_1 N \mathcal{D}[a_1^\dagger]\rho + \Gamma \mathcal{D}[a_0^\dagger a_1^2]\rho. \qquad (62)$$

Equation (62) is written in the interaction picture with respect to $H_0 = \omega_0 a_0^\dagger a_0 + \omega_1 a_1^\dagger a_1$, and the reduced density matrix ρ is $\rho = \text{Tr}_{\text{mode 2}}[W]$. The reduced collision Hamiltonian H_c is

$$H_c = V_{0000} a_0^\dagger a_0^\dagger a_0 a_0, \qquad (63)$$

and $\Gamma = 4|V_{0211}|^2/\kappa$. Consistently with Ref. [13] we call the limiting cases $\Gamma \ll \kappa_0$ and $\Gamma \gg \kappa_0$ the weak- and strong-pumping regimes, respectively.

A. Linearized fluctuation analysis

In order to obtain analytical approximations for the correlation functions

$$G_j^{(2)}(\tau) = \langle a_j^\dagger(0) a_j^\dagger(\tau) a_j(\tau) a_j(0)\rangle, \qquad (64)$$

and

$$D_j^{(2)}(\tau) = \langle a_j^\dagger(\tau) a_j(\tau) a_j^\dagger(0) a_j(0)\rangle \qquad (65)$$

in the two-mode system a linearized fluctuation analysis can be performed [10,18]. To this end the master equation (62) is converted to a Fokker-Planck equation using the P-function representation as described in [13]. This equation can be transformed to polar coordinates $\alpha_j = \sqrt{n_j} e^{i\phi_j}$, where α_j denotes the complex amplitudes originally appearing in the Fokker-Planck equation [19,20]. This leads to stochastic differential equations

$$dn_0 = [\Gamma n_1^2(n_0+1) - \kappa_0 n_0]dt + dS_{n_0}, \qquad (66)$$

$$dn_1 = [\kappa_1(N-n_1) - 2\Gamma n_1^2(n_0+1)]dt + dS_{n_1}, \qquad (67)$$

$$d\phi_0 = [-V_{0000}(2n_0-1) - V_{0101}n_1]dt + dS_{\phi_0}, \qquad (68)$$

$$d\phi_1 = [-V_{1111}(2n_1-1) - V_{0101}n_0]dt + dS_{\phi_1}. \qquad (69)$$

The correlation matrix for the stochastic forces $d\mathbf{S}^T = (dS_{n_0}, dS_{n_1}, dS_{\phi_0}, dS_{\phi_1})$ is given by

$$\mathbf{D} = \begin{pmatrix} 2\Gamma n_1^2 n_0 & -2\Gamma n_1^2 n_0 & -2V_{0000}n_0 & -V_{0101}n_0 \\ -2\Gamma n_1^2 n_0 & 2\kappa_1 N n_1 - 2\Gamma n_1^2 n_0 & -V_{0101}n_1 & -2V_{1111}n_1 \\ -2V_{0000}n_0 & -V_{0101}n_1 & \Gamma n_1^2/(2n_0) & \Gamma n_1/2 \\ -V_{0101}n_0 & -2V_{1111}n_1 & \Gamma n_1/2 & \dfrac{\kappa_1 N}{2n_1} + \dfrac{\Gamma n_0}{2} \end{pmatrix}. \qquad (70)$$

In the limit $n_0 \gg 1$ one obtains from Eqs. (66) and (67) the above-threshold semiclassical steady-state populations [13]

$$\bar{n}_0 = \frac{1}{2}\frac{\kappa_1}{\kappa_0}(N - \bar{n}_1), \qquad (71)$$

$$\bar{n}_1 = \sqrt{\frac{\kappa_0}{\Gamma}}, \qquad (72)$$

the threshold condition being $N > \sqrt{\kappa_0/\Gamma}$. The drift terms in Eqs. (66)–(69) and the correlation matrix $\mathbf{D}$ do not depend on the phases ϕ_j. This means that the time evolution of the atom numbers n_j is *not* influenced by the phase dynamics and is thus completely determined by Eqs. (66) and (67) alone. To proceed further we introduce the fluctuation variables $\delta n_j = n_j - \bar{n}_j$. In the linear approximation their time evolution is given by

$$d\,\delta\mathbf{n} = -\mathbf{k}\,\delta\mathbf{n}\,dt + d\mathbf{S}_n, \qquad (73)$$

where $\delta\mathbf{n}^T = (\delta n_0, \delta n_1)$ and the matrix $\mathbf{k}$ is obtained by linearizing the drift terms in Eqs. (66) and (67) around the steady-state values $\bar{n}_j$. The correlation matrix $\mathbf{D}_n$ for the stochastic forces $d\mathbf{S}_n^T = (dS_{n_0}, dS_{n_1})$ is given by the upper left 2×2 minor of the matrix $\mathbf{D}$ of Eq. (70) after replacing n_j by $\bar{n}_j$.

B. Second-order correlation function $G^{(2)}$

In the linear approximation the steady-state second-order correlation function for mode j is given by [10,18]

$$G_j^{(2)}(\tau) = (e^{-\mathbf{k}\tau}\boldsymbol{\sigma})_{jj} + \bar{n}_j^2 \qquad (74)$$

$(\tau \geq 0)$, where $\boldsymbol{\sigma}$ is the steady-state covariance matrix

$$\boldsymbol{\sigma} = \frac{\Delta \mathbf{D}_n + (\mathbf{k} - \Sigma)\mathbf{D}_n(\mathbf{k} - \Sigma)^T}{2\Sigma\Delta} \qquad (75)$$
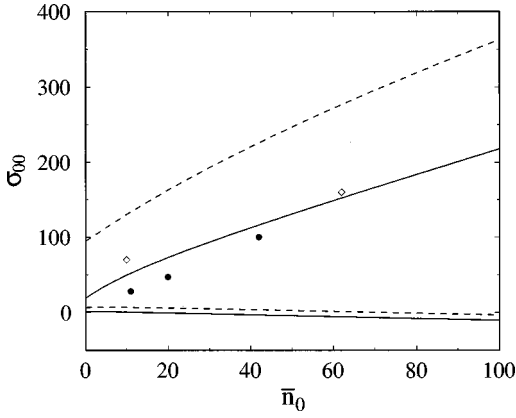
FIG. 2. Dependence of $\boldsymbol{\sigma}_{00}$ on $\bar{n}_0$. The curves are calculated using Eq. (76) for parameter values $\Gamma=0.07\kappa_0$ (ascending curves) and $\Gamma=15\kappa_0$ (descending curves), $\kappa_1=20\kappa_0$ (full), $\kappa_1=100\kappa_0$ (dashed). The single points show numerical results for $\Gamma=0.07\kappa_0$, $\kappa_1=20\kappa_0$ ($\bullet$), and $\kappa_1=100\kappa_0$ ($\diamond$), respectively.

with $\Delta=\det\mathbf{k}$ and $\Sigma=\text{Tr}\,\mathbf{k}$ (we use the numbers 0,1 as indices for the 2×2 matrices). For the matrix elements of $\boldsymbol{\sigma}$ one obtains the expressions

$$\boldsymbol{\sigma}_{00}=[\bar{n}_0^2(2\kappa_0-\kappa_0/\bar{n}_1)+\bar{n}_0(\kappa_1\bar{n}_1+\kappa_0+\kappa_1)$$
$$+\kappa_1^2\bar{n}_1/(4\kappa_0)]/(4\Gamma\bar{n}_1\bar{n}_0+\kappa_1), \qquad (76)$$

$$\boldsymbol{\sigma}_{11}=\frac{\kappa_0(2\bar{n}_1-1)\bar{n}_0+\kappa_1\bar{n}_1^2+\kappa_0\bar{n}_1}{4\kappa_0\bar{n}_0/\bar{n}_1+\kappa_1}, \qquad (77)$$

$$\boldsymbol{\sigma}_{01}=\boldsymbol{\sigma}_{10}=-\bar{n}_1/2. \qquad (78)$$

In the far-above-threshold limit $\bar{n}_0\gg1$ the covariances can be approximated as $\boldsymbol{\sigma}_{00}\approx\frac{1}{2}(\bar{n}_1-\frac{1}{2})\bar{n}_0$ and $\boldsymbol{\sigma}_{11}\approx\frac{1}{2}(\bar{n}_1-\frac{1}{2})\bar{n}_1$, respectively. For $\bar{n}_1>1/2$, i.e., in the weak-pumping regime, the second-order correlation functions thus show bunching, whereas for $\bar{n}_1<1/2$, i.e., in the strong-pumping regime, the linearized fluctuation analysis — which is, however, not expected to be fully reliable in that case — predicts antibunching. The normalized second-order correlation $g_0^{(2)}(0)$ $=G_0^{(2)}(0)/\bar{n}_0^2$ goes to 1 with $1/\bar{n}_0$ for large $\bar{n}_0$. In contrast, $g_1^{(2)}(0)\rightarrow3/2-1/(4\bar{n}_1)$. For the case of $\bar{n}_1\gg1$ the results for $\boldsymbol{\sigma}_{00}$ and $\boldsymbol{\sigma}_{11}$ are in agreement with the conclusions of Ref. [13]. To illustrate the physical contents of Eqs. (76) and (77) in Fig. 2 the dependence of $\boldsymbol{\sigma}_{00}$ on $\bar{n}_0$ is shown for the weak- and strong-pumping regime and different values of κ_1.

An expansion of $e^{-\mathbf{k}\tau}$ in the parameter $\bar{n}_0/\bar{n}_1$ yields the approximate result

$$G_j^{(2)}(\tau)=\boldsymbol{\sigma}_{jj}e^{-q_j\tau}+\bar{n}_j^2 \qquad (79)$$

for the time dependence of the correlation functions (74). Thereby, the q_j are the two eigenvalues of the matrix $\mathbf{k}$. For $\bar{n}_0/\bar{n}_1>1$ they are approximately given by

$$q_0=\frac{4\kappa_0^2}{4\kappa_0+\kappa_1\bar{n}_1/\bar{n}_0}, \qquad (80)$$

$$q_1=\kappa_1+4\kappa_0\bar{n}_0/\bar{n}_1. \qquad (81)$$

Their inverses can be interpreted as the relevant time scales for the dynamics of the atom number fluctuations. Numerical comparison to Eq. (74) shows that the approximation (79) is very accurate, in general. The time dependence of the second-order correlation functions is thus purely exponential. The correlation function $G_0^{(2)}$ decays on a time scale of the order of κ_0, whereas the time evolution of $G_1^{(2)}$ is much more rapid.

C. Density-correlation function $D^{(2)}$

Using Eq. (10.5.28) of Ref. [19] we find that in the linear approximation the steady-state density-correlation function $D_j^{(2)}$ for mode j is given by

$$D_j^{(2)}(\tau)=\bar{n}_j(e^{-\mathbf{k}\tau})_{jj}+G_j^{(2)}(\tau). \qquad (82)$$

From Eqs. (76) and (77) it follows that $D_j^{(2)}(0)>\bar{n}_j^2$. In analogy to Eq. (79) one obtains the expression

$$D_j^{(2)}(\tau)=(\bar{n}_j+\boldsymbol{\sigma}_{jj})e^{-q_j\tau}+\bar{n}_j^2 \qquad (83)$$

for the explicit time dependence of $D_j^{(2)}$. The intensity fluctuation spectrum, i.e., the Fourier transform of $D_j^{(1)}(\tau)-\bar{n}_j^2$, is thus a Lorentzian.

It should be noted that all results of this section are independent of the rate of elastic collisions (as quantified by V_{0000}) between atoms in the laser mode. This means that in the two-mode description the atom laser is second-order coherent [at least in the sense of $g_0^{(2)}(\tau)\approx1$ for all τ] even if V_{0000} is large. In such cases the first-order correlation function $G^{(1)}$ will decay very rapidly so that the laser is not first-order coherent, and is characterized by a large linewidth [17].

D. Numerical examples

As discussed in detail in Ref. [16], the master equations (58) and (62) may be solved numerically with the help of quantum Monte Carlo techniques [21,22]. The correlation functions $G^{(2)}$ and $D^{(2)}$ can be calculated within this approach according to the description given in Ref. [22]. In the following we compare some numerical results with the analytical predictions of Secs. IV B and IV C.

Strong-pumping regime. Figure 3(a) depicts a typical result for the calculation of $D_0^{(2)}$ and $G_0^{(2)}$ in the strong-pumping regime. In this example, the parameters $\Gamma=15\kappa_0$, $\kappa_1=20\kappa_0$, and $N=1.2$ were chosen yielding a numerical equilibrium population of $\bar{n}_0=9.0$ (9.4 analytically). As should be expected, $D_0^{(2)}(0)-G_0^{(2)}(0)\approx\bar{n}_0$. The behavior of $D_0^{(2)}(\tau)$ is very well approximated by an exponential decay with time constant $1/q_0$, as predicted in Eq. (83). From the behavior of $G_0^{(2)}(\tau)$ it can be inferred that $|g_0^{(2)}(\tau)-1|\ll1$ for all τ. However, even after a very large number of Monte
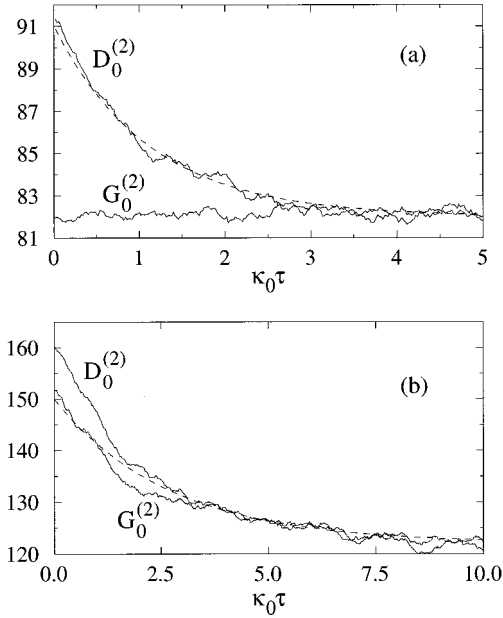
FIG. 3. Numerical calculation of $D_0^{(2)}(\tau)$ and $G_0^{(2)}(\tau)$ for parameter values $\Gamma = 15\kappa_0$, $\kappa_1 = 20\kappa_0$, $N = 1.2$ (a) and $\Gamma = 0.07\kappa_0$, $\kappa_1 = 20\kappa_0$, $N = 3.9$ (b). Dashed curves: exponential decay with corresponding time constant $1/q_0$.

Carlo simulations, numerical noise prevents any further details of the time dependence of $G_0^{(2)}(\tau)$ to be identified. This observation applies to most calculations in the strong-pumping regime. In particular, it could not be unambiguously determined whether antibunching actually occurs for larger values of $\bar{n}_0$. On the other hand, these numerical results are compatible with the fact that Eq. (76) predicts a small value of $|g_0^{(2)}(\tau) - 1|$ (compare with Fig. 2).

It should be noted that a small amount of antibunching in $G_0^{(2)}$ could be observed in calculations for the three-mode model in cases in which V_{0000} is large compared to V_{0211}. Under these conditions, however, the main effect to be observed is a significant decrease in the equilibrium population $\bar{n}_0$.

Weak-pumping regime. In contrast to the previous case, for the weak-pumping regime it can be expected on the grounds of the linear analysis that $g_0^{(2)}(0)$ is significantly different from 1 if $\bar{n}_0$ is not too large (cf. Fig. 2). As exemplified in Fig. 3(b), this prediction is indeed confirmed by the numerical calculations. There the correlation functions $D_0^{(2)}$ and $G_0^{(2)}$ are shown for the parameter values $\Gamma = 0.07\kappa_0$, $\kappa_1 = 20\kappa_0$, and $N = 3.9$. Unfortunately, the quantitative results of the linear analysis in the weak-pumping regime are not very accurate for low values of $\bar{n}_0$ (to which the numerical computations have to be restricted due to time constraints). For example, for the above parameters Eq. (71) yields $\bar{n}_0 = 1.2$, which is much smaller than the numerical value of 11. However, Eq. (80) still constitutes a good approximation to the decay rate of the correlation functions if it is used with the numerically determined values of $\bar{n}_0$ and $\bar{n}_1$. This is demonstrated by the dashed curve in Fig. 3(b), which depicts an exponential decay with a time constant calculated
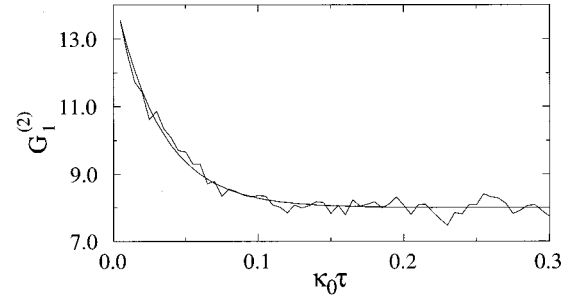

FIG. 4. Numerical calculation of $G_1^{(2)}(\tau)$ for parameter values $\Gamma = 0.07\kappa_0$, $\kappa_1 = 20\kappa_0$, $N = 3.9$. Dashed curve: exponential decay with time constant $1/q_1$.

in this way. A similar agreement was also found in other examples.

In Fig. 2 the results of several numerical calculations of $\bar{\sigma}_{00}$ are shown as a function of the numerical value of $\bar{n}_0$ for the parameters $\Gamma = 0.07\kappa_0$, $\kappa_1 = 20\kappa_0$ ($\bullet$), and $\kappa_1 = 100\kappa_0$ ($\diamondsuit$). The numerical values of σ_{00} should be understood as having an error margin of at least $\pm$ 10-15%. The results depicted agree in order of magnitude with the predictions of Eq. (76) and also demonstrate a dependence of σ_{00} on $\bar{n}_0$ and κ_1 similar to the analytical one.

Second-order correlation function for the pumping mode. An example of the behavior of the second-order correlation function $G_1^{(2)}(\tau)$ in the weak-pumping limit is shown in Fig. 4. There, the parameter values $\Gamma = 0.07\kappa_0$, $\kappa_1 = 20\kappa_0$, and $N = 3.9$ were used. The order of magnitude of $G_1^{(2)}(0)$ as well as the temporal decay rate of $G_1^{(2)}$ (which is much larger than the decay rate of $G_0^{(2)}$) are in good agreement with the analytical predictions. It should be noted that the time evolution of the mean population of the pumping mode $\langle a_1^\dagger(t) a_1(t) \rangle$ starting from an initial vacuum state contains both characteristic time scales $1/q_0$ and $1/q_1$. This is quite different from the behavior of $G_1^{(2)}$, which is characterized by $1/q_1$ alone. In the strong pumping limit the time dependence of $G_1^{(2)}$ could again not be recognized due to numerical noise. This is consistent with the fact that the linearized fluctuation analysis predicts a small value of $|g_1^{(2)}(0) - 1|$ for the parameter values investigated. Furthermore, the calculations indicated that Eq. (72) ceases to be valid for large Γ. It was not possible to reduce $\bar{n}_1$ to very small values in which case a more pronounced antibunching would be expected.

In conclusion, we see that the results obtained from the linear fluctuation analysis describe well the essential aspects of the behavior of the correlation functions $D_0^{(1)}$ and $G_0^{(2)}$ and may be used as a first quantitative estimate.

VI. CONCLUSION AND OUTLOOK

In this paper, we have adopted an operational approach to introduce several classes of coherence of the Schrödinger field. Of particular importance are density coherence, which is connected to far-off-resonance imaging measurements, and field coherence, which can be measured in ionization-type measurements. One can readily imagine further classes of coherence associated with other types of measurements,

but they are probably not as important as field and density coherence.

One question of considerable significance in the future will be to quantify the usefulness of various sources of Schrödinger fields for specific applications. In optics, one of the most important characteristic of lasers is their spectral width, and higher-order coherence plays a limited role in most cases. By analogy, past studies of atom lasers have concentrated on their spectral width, as determined by their first-order field correlations. It has been found that this linewidth can be quite broad, especially in the presence of elastic collisions. Indeed, things can be so bad that the atom laser linewidth is broader than the natural linewidth of the atom cavity, in sharp contrast to the optical situation where, of course, the reverse is true. It is not clear, however, whether this is a useful way to determine the quality and usefulness

of an atom laser. While this is likely to be the case in some interferometric applications, other possible uses of atom laser beams, such as coherent lithography, may well require only a high degree of density coherence, in which case, as we have seen, elastic collisions do not play a detrimental role. Hence, we believe that it is important at this point to start analyzing in detail the coherence requirements of specific atom laser applications, so as to optimize their design.

---

[1] R. Glauber, in *Quantum Optics and Electronics*, edited by C. de Witt, A. Blandin, and C. Cohen-Tannoudji (Gordan and Breach, New York, 1965).

[2] E. V. Goldstein and P. Meystre, Phys. Rev. Lett. **80**, 5036 (1998).

[3] K. B. Davis, M.-O. Mewes, M. R. Andrews, N. J. van Druten, D. S. Durfee, D. M. Kurn, and W. Ketterle, Phys. Rev. Lett. **75**, 3969 (1995).

[4] J. Javanainen, Phys. Rev. Lett. **75**, 1927 (1995).

[5] J. E. Thomas and L. J. Wang, Phys. Rev. A **49**, 558 (1994).

[6] J. E. Thomas and L. J. Wang, Phys. Rep. **262**, 311 (1995).

[7] C. Cohen-Tannoudji, J. Dupont-Roc, and G. Grynberg, *Atom-Photon Interactions: Basic Processes and Applications* (Wiley, New York, 1992).

[8] E. M. Wright, D. F. Walls, and J. C. Garrison, Phys. Rev. Lett. **77**, 2158 (1996).

[9] E. M. Lifshitz and L. P. Pitaevskii, *Statistical Physics, Part 2* (Pergamon Press, New York, 1980).

[10] D. F. Walls and G. J. Milburn, *Quantum Optics* (Springer-Verlag, Berlin, 1994).

[11] R. J. Dodd, C. W. Clark, M. Edwards, and K. Burnett, Opt. Express. **1**, 284 (1997).

[12] A. Guzman, M. Moore, and P. Meystre, Phys. Rev. A **53**, 977 (1996).

[13] H. Wiseman, A. Martins, and D. F. Walls, Quantum Semiclassic. Opt. **8**, 737 (1996).

[14] M. Holland, K. Burnett, C. Gardner, J. I. Cirac, and P. Zoller, Phys. Rev. A **54**, R1757 (1996).

[15] M. Moore and P. Meystre, Phys. Rev. A **56**, 2989 (1997).

[16] M. Moore and P. Meystre, J. Mod. Opt. **44**, 1815 (1997).

[17] O. Zobay and P. Meystre, Phys. Rev. A **57**, 4710 (1998).

[18] P. Meystre and M. Sargent III, *Elements of Quantum Optics* (Springer-Verlag, Berlin, 1991).

[19] C. W. Gardiner, *Handbook of Stochastic Methods* (Springer-Verlag, Berlin, 1983).

[20] C. W. Gardiner, *Quantum Noise* (Springer-Verlag, Berlin, 1991).

[21] R. Dum, A. S. Parkins, P. Zoller, and C. W. Gardiner, Phys. Rev. A **46**, 4382 (1992).

[22] K. Mølmer, Y. Castin, and J. Dalibard, J. Opt. Soc. Am. A **10**, 524 (1993).